Received: 19 September 2022 | Revised: 30 October 2022 | Accepted: 11 November 2022

DOI: 10.1002/elps.202200228

ELECTROPHORESIS

RESEARCH ARTICLE

Combining amperometry and mass spectrometry as a dual detection approach for capillary electrophoresis

Daniel Böhm | **Martin Koall** | **Frank-Michael Matysik**

Institute of Analytical Chemistry, Chemo- and Biosensors, University of Regensburg, Universitätsstraße 31, Regensburg, Germany

Correspondence
Frank-Michael Matysik, Institute of Analytical Chemistry, Chemo- and Biosensors, University of Regensburg, Universitätsstraße 31, 93053 Regensburg, Germany.
Email: frank-michael.matysik@chemie.uni-regensburg.de

Color online: See the article online to view Figures 1–5 in color.

Funding information
Deutsche Forschungsgemeinschaft (DFG, German Research Foundation), Grant/Award Number: MA1491/12-1

Abstract

Dual detection concepts (DDCs) are becoming more and more popular in analytical chemistry. In this work, we describe a novel DDC for capillary electrophoresis (CE) consisting of an amperometric detector (AD) and a mass spectrometer (MS). This detector combination has a good complementarity as the AD exhibits high sensitivity, whereas the MS provides excellent selectivity. Both detectors are based on a destructive detection principle, making a serial detector arrangement impossible. Thus, for the realization of the DDC, the CE flow was divided into two parts with a flow splitter. The DDC was characterized in a proof-of-concept study with ferrocene derivates and a nonaqueous background electrolyte. We could show that splitting the CE flow was a suitable method for the instrumental realization of the DDC consisting of two destructive detectors. By lowering the height of the AD compared to the MS, it was possible to synchronize the detector responses. Additionally, for the chosen model system, we confirmed that the AD was much more reproducible and had lower limits of detection (LODs) than the MS. The LODs were identical for the DDC and the single-detection arrangements, indicating no sensitivity decrease due to the CE flow splitting. The DDC was successfully applied to determine the drug and doping agent trimetazidine.

KEYWORDS
amperometric detection, capillary electrophoresis, dual detection concept, flow splitting, mass spectrometry

1 | INTRODUCTION

The number of complex samples in fields like medicine or environmental research is steadily increasing. Therefore, powerful separation and detection methods are required [1, 2]. After its invention by Jorgenson and Lukacs [3] in the early 1980s, capillary electrophoresis (CE) became an established separation method due to its high separation efficiency, short analysis times, and low sample

Abbreviations: AD, amperometric detection; CE-AD, capillary electrophoresis–amperometric detection; CE-AD/MS, capillary electrophoresis–amperometric detection and mass spectrometry; CE-MS, capillary electrophoresis–mass spectrometry; DDC, dual detection concept; FcMeOH, ferrocenemethanol; $[FcMTMA]^+$, (ferrocenylmethyl)trimethylammonium ion; FS, flow splitter; TMZ, trimetazidine.

consumption [4–6]. Due to the minimal amount of injected sample and the small dimensions in CE, the sensitivity of the detection technique plays an important role. A detection method that copes very well with these conditions is amperometric detection (AD). AD was first applied with CE by Wallingford and Ewing [7] in 1987 by a porous joint as an electrical field decoupler. A few years later Ewing's group also introduced the first hyphenation of CE with AD without an electrical field decoupler termed end-column AD [8]. For electroactive analytes, AD is considered as a very sensitive detection method [9–11]. In combination with a nonaqueous background electrolyte (BGE), the long-term stability of AD is excellent, allowing the quantification utilizing external calibration or standard addition method [12, 13]. Nevertheless, one drawback of AD is the limited selectivity. With AD, it is usually impossible to identify unknown substances or to examine the peak purity. In contrast to AD, mass spectrometry (MS) is the detection method of choice when it comes to selectivity because it is possible to determine molecular weight and structural information [14]. Smith and coworkers [15] described the combination of electrospray ionization (ESI) and MS as a detection method for CE in 1987. The sensitivity of ESI-MS depends strongly on the ionization efficiency of the analyte. Additionally, the sensitivity of ESI-MS is negatively affected by the dilution of the CE effluent with sheath liquid of the sheath-flow interface. Thus, the limits of detection (LODs) of ESI-MS are usually higher than the ones determined with AD [11, 16–18]. Moreover, the long-term stability of ESI-MS signals is typically relatively poor. Therefore, the quantification with ESI-MS is often achieved with isotope-labeled internal standards, but these are expensive and not available for all analytes [16–19].

A dual detection concept (DDC) combines the power of different single-detection techniques and overcomes their limitations. Both detectors (AD and MS) have an excellent complementarity; therefore, they provide a powerful DDC, which is to the best of our knowledge not described in literature so far. According to the features of the detectors, the AD is perfect for quantifying substances, and the MS is ideal for identifying substances. In recent years, many DDCs for CE were developed [20–25]. These DDCs consist of at least one nondestructive detector. This simplifies the instrumental realization because a serial detector arrangement could be used [2]. The development of the novel DDC (CE-AD/MS) is much more challenging because both detectors are destructive and must be decoupled from the high voltage field of the CE. For the realization of this concept, the CE flow has to be split into two parts; thereby, it is possible to arrange the detectors in parallel to each other. The splitting of the CE flow is already described in literature but predominately in the context of 2D separations or for the concurrent analysis of cations and anions [26–28]. Böhm et al. [29] presented a user-friendly flow splitter (FS) that could be used for flow splitting in CE. Different types of FSs were characterized. Additionally, it was demonstrated that the FSs introduced no peak broadening wherefore the splitting was considered to be dead volume-free. Based on these results, we used this FS for the realization of the new DDC. In principle, an approach with two capillaries (both capillaries starting from the inlet vial and one capillary going to the AD and the other to the MS) would also be possible. This approach was not used to implement the DDC because each capillary has its characteristics, which leads to different migration behavior, making a synchronization of the migration times difficult. Additionally, a two capillary approach cannot be implemented with most of the commercially available CE devices.

In this proof-of-concept study, we describe the development of a DDC for CE combining AD and MS. For the characterization of the new DDC ferrocene derivates dissolved in a nonaqueous BGE were used. The nonaqueous BGE was favorable for both detectors. On the one hand, it has a wide potential window and an excellent long-term stability in terms of AD. On the other hand, the nonaqueous BGE is very volatile, which is good for ESI-MS [30]. Finally, we determined trimetazidine (TMZ), which was recently discussed in the context of doping, demonstrating the complementary action of AD/MS.

2 | MATERIALS AND METHODS

2.1 | Chemicals and materials

The following chemicals were used, all of analytical grade: acetonitrile (ACN), ammonium acetate, 0.1 M sodium hydroxide solution, formic acid, and ultrapure water provided by a Milli-Q Advantage A10 system, were acquired from Merck (Darmstadt, Germany). Ferrocenemethanol (FcMeOH) was purchased from ABCR (Karlsruhe, Germany). (Ferrocenylmethyl)trimethylammonium iodide ([FcMTMA]I) was obtained from Strem Chemicals (Newburyport, USA). Acetic acid was purchased from Carl Roth (Karlsruhe, Germany). Trimetazidine dihydrochloride (TMZ) and 2-propanol were purchased from Sigma-Aldrich (St. Louis, USA). Fused silica capillaries (50 µm inside diameter, 365 µm outside diameter, polyimide coated) were received from Polymicro Technologies (Phoenix, USA). The FS CapTite Interconnect Y C360-203Y-U-C100 and the corresponding fitting CapTite One-Piece Fitting C360-100 were obtained from LabSmith (Livermore, USA).

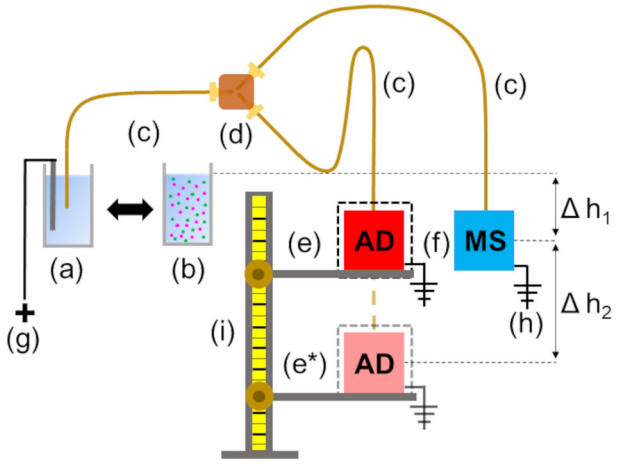

FIGURE 1 Scheme of the CE-AD/MS setup showing the main components: Inlet vial (a), sample vial (b), fused silica capillaries (c), FS (d), AD (e), MS (f), positive high voltage power source (g), grounding (h), and Faraday cage with integrated stand (i). There was a permanent height difference Δh_1 between the inlet vial and the MS of 6 cm. The height difference Δh_2 between AD and MS was variable. The height difference Δh_2 was adjusted by lowering the AD (e*).

2.2 | Instrumentation CE-AD/MS

Figure 1 shows a scheme of the DDC (CE-AD/MS), consisting of a CE device connected to an AD and an MS via a Y-shaped FS. For a better illustration, a photograph of the DDC is shown in Figure S1. The laboratory-constructed CE system was connected to a positive high voltage power supply from ISEG (Radeberg, Germany). Special caution is required when experiments are performed with high voltage. The CE device was placed in a safety housing that was equipped with safety switches and warning signs.

The end-column AD was also laboratory-constructed and is described in detail elsewhere [13]. Briefly, the AD was made of polytetrafluoroethylene, which allowed the usage in combination with the ACN-based BGE. For the user-friendly positioning of the capillary and the working electrode, the AD was equipped with two symmetrically arranged stainless steel tubes which served as a guiding system. The separation capillary and the working electrode were placed at a distance of 50 µm from each other. The positioning was done utilizing an UltraZoom Pro digital microscope from dnt (Dietzenbach, Germany). The working electrode consisted of a 25 µm platinum wire sealed in a glass tube and the Ag/AgCl reference electrode (filled with BGE) was placed in the cap of the AD. A stainless steel tube served additionally as counter electrode for the AD and as grounding for the electrophoretic circuit of the CE. The electrodes were connected to an SP-200 potentiostat equipped with an ultralow current module from BioLogic (Seyssinet-Pariset, France). The AD cell was filled with BGE and placed in a Faraday cage to reduce electromagnetic interference effects. As in this work an AD with an end-column design was used, the potential shift at the working electrode was determined at the beginning of each measurement day by performing cyclic voltammograms without and with 25 kV separation voltage. The potentials of the electrode pretreatment protocol and the detection potential were corrected by the potential shift. The determination of the potential shift for NACE in combination with an end-column AD is in detail described elsewhere [31]. Simultaneously to each CE measurement, an electrode pretreatment protocol (2.5 V for 10 s followed by −0.5 V for 10 s) was started to avoid electrode fouling. Subsequently, the detection potential (0.8 V for the ferrocene derivates and 1.3 V for the TMZ) was applied at the working electrode.

A micrOTOF-MS from Bruker Daltonics (Bremen, Germany) with a coaxial sheath liquid ESI interface from Agilent Technologies (Santa Clara, USA) was used as a second detector. Due to the properties of the analytes, all measurements were performed in the positive MS mode. For the measurements, the following MS parameters were used: nebulizer gas pressure 1 bar, electrospray voltage 4 kV, dry gas (N_2) flow 4 L/min, dry gas temperature 190°C, end plate offset −500 V, capillary exit 85 V, skimmer 1 29 V, skimmer 2 23 V, hexapole 1 23 V, hexapole RF 80 Vpp, lens 1 transfer 35 µs, lens 1 pre pulse storage 6 µs, m/z 50–400, and spectra acquisition rate 5 Hz. The sheath liquid had a flow rate of 8 µl/min and consisted of water, 2-propanol, and formic acid (49.9:49.9:0.2, v/v/v).

A Y-shaped FS (material polyetherimide, dead volume 9 nl, and thru-hole diameter 100 µm) was used to split the CE flow. A microscopic image and a detailed description of the FS can be found in our previous manuscript [29]. The FS was connected to three capillary pieces. The capillary piece on the injection side had a length of 30 cm, and the two capillary pieces on the detection side had a length of 35 cm. On both sides of the capillary pieces, about 3 mm of the polyimide coating was removed with a razor blade to avoid any dead volume introduced by polyimide swelling. To prevent a dead volume introduced by nonplanar capillary tips, all capillary edges were polished at a 90° angle with an abrasive paper of 30 and 3 µm grid size. Before the first CE measurements, the capillaries were conditioned by flushing them for 10 min with 0.1 mM sodium hydroxide solution, followed by 5 min with ultrapure water and at least 30 min with BGE.

There was a fixed height difference of 6 cm between the capillary inlet and the tip of the coaxial sheath liquid ESI interface of the MS. The AD was variable in height. For some measurements, it was located at the same height as

the tip of the coaxial sheath liquid interface of the MS, but for synchronizing the detector responses the AD was placed at a lower height level. To simplify the height adjustment, the AD was placed in a stand that was integrated into the Faraday cage. The Faraday cage with an integrated stand is shown in Figure S1. The injection was performed hydrodynamically by the height difference between the injection side and the detectors. The suction pressure of the ESI source also supported the injection. The optimized injection time was 20 s. For all measurements, a separation voltage of 25 kV was applied.

2.3 | Experimental parameters and sample preparation

All experiments were performed with a nonaqueous BGE consisting of 10 mM ammonium acetate and 1 M acetic acid in ACN. If not indicated differently, a sample solution containing 0.1 mM $[FcMTMA]^+$ and 0.5 mM FcMeOH in BGE was used to characterize the DDC. The effect of the height difference between AD and MS was investigated to achieve similar migration times for both detectors. For the very first measurements, both detectors were at the same level, defined as a height difference of 0 cm. As the height of the MS was not adjustable, the height of the AD was systematically decreased by 2 cm steps compared to the tip of the coaxial sheath liquid interface of the MS. The height difference was adjusted for all subsequent measurements to get a simultaneous detector response. The reproducibility of the most important parameters like migration time, peak areas, and peak heights was tested by performing 11 consecutive measurements of the sample solution. To evaluate a possible decrease in detectability due to the flow splitting, the LODs for the DDC and the single-detection arrangements were determined. For the single-detection measurements, each detector (AD and MS) was separately coupled with the CE device. For these measurements, almost all parameters were retained. Only the capillary length and the injection times for the measurements with the single-detection arrangements were adjusted. The CE device was coupled to the single detectors via a continuous capillary with a length of 65 cm. The injection times were optimized for each single-detection arrangement to ensure maximum sensitivity. The optimized injection times for the DDC (CE-AD/MS) and the single-detection arrangement (CE-AD) were 20 s, for the other single-detection arrangement (CE-MS) the injection time was 15 s.

In the second set of experiments, TMZ was used as an analyte. The electrochemical behavior of TMZ was characterized by cyclic voltammetry. The cyclic voltammograms were performed in a batch cell with identical electrodes to the AD. A solution of 0.1 mM TMZ in bare BGE was used for the cyclic voltammograms. The cyclic voltammograms were measured between 0 and 1.5 V with a scan rate of 50 mV/s. For the CE-AD/MS measurements, a sample solution containing 1.25 µg/ml TMZ in BGE, including 10% MeOH was used. The MeOH was added to increase the solubility of the TMZ in BGE.

All LODs (ferrocene derivates and TMZ) were determined by measuring the detector signals within a concentration range near the LOD. The LODs were determined for an S/N of three, and each measurement was performed three times.

2.4 | Data evaluation

The measurement data were evaluated with Origin 2020 SR 1 from OriginLab (Northampton, USA), Excel 2016 from Microsoft (Redmond, USA), Data Analysis 4.0 SP1 from Bruker Daltonics (Bremen, Germany), and EC-Lab V11.43 from BioLogic (Seyssinet-Pariset, France).

3 | RESULTS AND DISCUSSION

3.1 | Synchronization of the detector responses

For the first proof-of-concept measurements with the new DDC, we used a model system consisting of $[FcMTMA]^+$ as cationic model analyte and FcMeOH as electroosmotic flow (EOF) marker. These analytes were very favorable for the characterization of the DDC because they could be detected with both detectors (AD and MS). The m/z 199 was used for the MS as it was the most sensitive signal for both model analytes ($[FcMTMA]^+$ and FcMeOH).

For the first measurements, the detectors were placed at the same height. This means the AD and the tip of the coaxial sheath liquid interface of the MS were at the same height level. The corresponding electropherograms measured with the AD are shown on top, and the MS measurements are shown in Figure 2A. The model analytes could be detected at both detectors. This shows that the splitting of the CE flow for the implementation of a new DDC worked. For no height difference between the detectors, it was found that the model substances migrated to the side of the MS earlier than at the side of the AD. The reason for this finding was the suction pressure of the ESI interface, which accelerated the flow toward the MS. In order to utilize the full potential of the DDC, it is desirable to synchronize the migration times as it is planned to identify the substances via MS and simultaneously

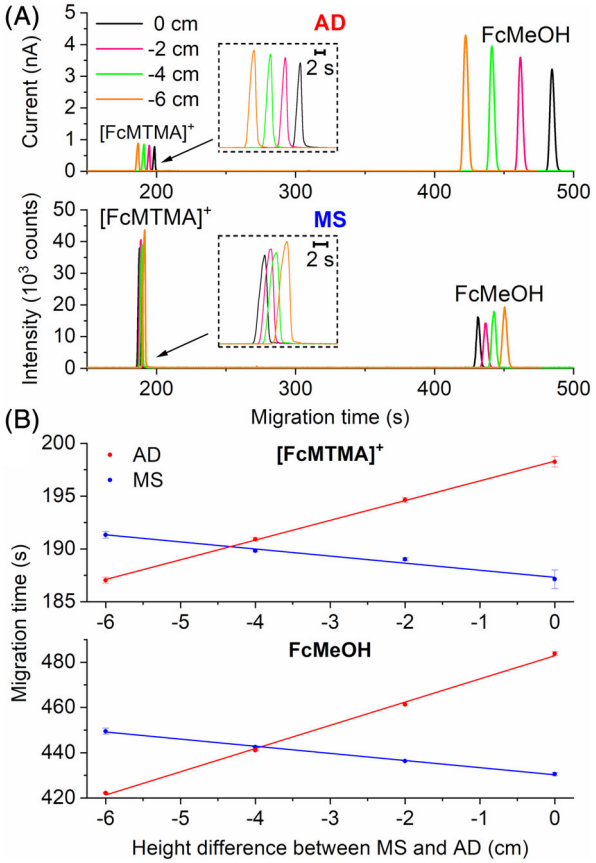

FIGURE 2 (A) CE-AD/MS measurements of the model mixture $[FcMTMA]^+$/FcMeOH for different height differences (0, −2, −4, and −6 cm) between AD and MS. The electropherograms were recorded with AD (top) and with MS (bottom). Corresponding electropherograms for the AD and the MS have the same color. (B) Development of the migration times for $[FcMTMA]^+$ (top) and FcMeOH (bottom) depending on the height difference between AD and MS. Experimental parameters: 0.1 mM $[FcMTMA]^+$ and 0.5 mM FcMeOH in BGE, injection time 20 s, separation voltage 25 kV, detection potential AD 0.8 V (vs. Ag/AgCl), and extracted ion electropherograms for both model analytes (m/z 199). The detectors were placed after a respective total capillary length of 65 cm (30 cm in front of the FS and 35 cm behind the FS).

quantify the substances via AD. It would be ideal if the detector responses could be synchronized without internal standards and mathematical calculations. Therefore, we tried to synchronize the detector responses by adjusting the height difference between the two detectors. By lowering the AD, the hydrodynamic flow toward the AD was increased, which could compensate the suction pressure of the ESI interface at the MS. The effect on the migration time for a reduction of the height level of the AD compared to the MS is depicted in Figure 2A. For a height difference of −2 cm, the substances migrated earlier at the side of the AD and later at the side of the MS compared to the first measurements where the detectors were at the same height. This trend continued with increasing height differences. For a height difference of −6 cm, the substances migrated even earlier on the side of the AD than on the MS side. Due to these findings, there should be a height difference where the substances migrate simultaneously at both detectors. We plotted the migration times against the height differences for both model analytes to find the ideal height difference for simultaneous detection. The corresponding chart for the cationic model analyte ($[FcMTMA]^+$) is depicted on top and for the EOF marker (FcMeOH) at the bottom of Figure 2B. It was found that there was a linear correlation between migration times and height differences. There was an intercept between the linear trend curves of the AD and the MS at about −4 cm, indicating that for this height difference, the substances migrated simultaneously at both detectors. The synchronization of the migration times was stable throughout the whole measurement day. When the capillaries were not disassembled from the detectors overnight, no or only minimal adjustments had to be done before the next measurements session. The height difference for all subsequent measurements was adjusted to get a simultaneous detector response.

3.2 | Reproducibility of the DDC (CE-AD/MS)

As it was possible to synchronize the detectors by a simple adjustment of the height difference between AD and MS, as a next step we looked at the reproducibility of the new DDC. The reproducibility was tested by performing 11 consecutive measurements. The corresponding electropherograms are shown in Figure 3 . It could be seen that the substances migrated nearly simultaneously at both detectors due to the height adjustment carried out at the beginning of the measurements. For both detectors, it was found that all peaks showed a nearly Gaussian shape with negligible peak tailing. For the AD one peak looked like the other, whereas for the MS some differences in the peak shape were detectable. To substantiate this finding, we determined the peak areas and heights for the two different detectors and summarized the figures of merit in Table 1. It was found that the RSDs of the peak areas were in a range of 1.2%–1.3% for the AD and 6.9%–10.8% for the MS. A similar result was found for the peak heights, where the RSDs were in the range of 0.4%–0.7% for the AD and between 6.3% and 10.0% for the MS. Both results showed that the reproducibility was better for the AD than for the MS. As the reproducibility of the detector response is especially important for the quantification of analytes, we concluded that the AD was better suited for quantification purposes than the MS. Due to the excellent reproducibility of the

TABLE 1 CE-AD/MS studies of 0.1 mM $[FcMTMA]^+$ and 0.5 mM FcMeOH for the determination of the reproducibility of the migration time (t), the peak area (A), the peak height (H), and the corresponding SDs at the different detectors ($n = 11$)

Species	$[FcMTMA]^+$		FcMeOH	
Detector	AD	MS	AD	MS
t (s)	191.1 ± 0.2	190.2 ± 0.3	450.2 ± 0.5	452.3 ± 0.8
A (pA•s or counts•s)	$156 \cdot 10^1 \pm 2 \cdot 10^1$	$58 \cdot 10^3 \pm 4 \cdot 10^3$	$163 \cdot 10^2 \pm 2 \cdot 10^2$	$37 \cdot 10^3 \pm 4 \cdot 10^3$
H (pA or counts)	893 ± 4	$32 \cdot 10^3 \pm 2 \cdot 10^3$	$409 \cdot 10^1 \pm 3 \cdot 10^1$	$10 \cdot 10^3 \pm 1 \cdot 10^3$

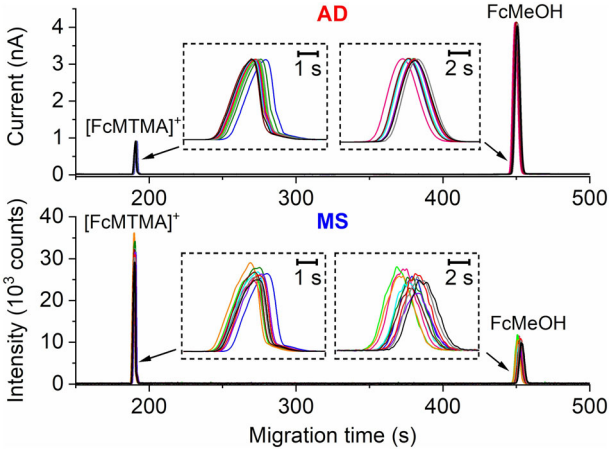

FIGURE 3 CE-AD/MS measurements of the model mixture $[FcMTMA]^+$/FcMeOH for 11 consecutive measurements. The electropherograms on top were recorded with AD and at the bottom with MS. Corresponding electropherograms for the AD and the MS have the same color. Experimental parameters: The conditions are as in Figure 2.

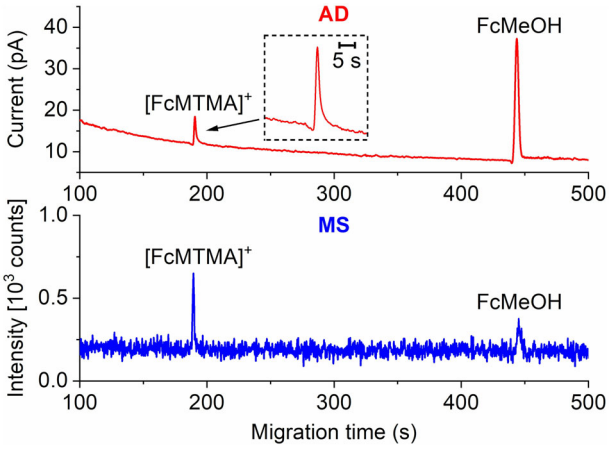

FIGURE 4 CE-AD/MS measurement of the model mixture containing 1 µM $[FcMTMA]^+$ and 10 µM FcMeOH in BGE. The electropherograms on top were recorded with AD (red) and at the bottom with MS (blue). Experimental parameters: the conditions are as in Figure 2.

AD, it could be used in combination with external calibration or standard addition methods. There is no need for an internal standard that is often used in combination with MS. Summing up, if the analytes can be detected with both detectors, the AD should be used for quantification and the MS for identification. Furthermore, the small RSDs of the AD also showed the good reproducibility of the CE flow splitting. This was an essential point, because, for the quantification, it was important that the split ratio was stable throughout the measurements. In one of our previous works, we also found a good reproducibility of the CE flow splitting for the used FS [29].

3.3 | Detectability characteristics of the DDC (CE-AD/MS)

Another point addressed in this study was the detectability within the new DDC. Before the first measurements, the injection time was optimized to get the maximum peak height with no plateau formation for the lowest LODs. The LODs of the dual detection method (CE-AD/MS) were determined for an S/N of 3 and are listed in Table 2. The LODs were up to a factor of 60 for $[FcMTMA]^+$ and 1357 for FcMeOH lower for the AD than for the MS. It was striking that the differences in LODs between the two detectors were higher for FcMeOH than for $[FcMTMA]^+$. This finding was because $[FcMTMA]^+$ was already positively charged and can therefore be easily detected by MS. Therefore, for $[FcMTMA]^+$ the differences between the LODs of the AD and the MS were smaller. In contrast, the LODs for FcMeOH were much lower for the AD compared to the MS, as FcMeOH has a poor ionization efficiency. If the substances can be detected with MS and AD, the AD has usually the lower LODs. To illustrate the excellent detectability of the AD in comparison to the MS, we performed measurements with model analyte concentrations near the LODs of the MS. The corresponding electropherograms are depicted in Figure 4. From the electropherograms, one could see that the S/Ns were relatively low for the MS and much higher for the AD. Nevertheless, it was possible to identify the substances using MS.

To see if there was a decrease in detectability for the DDC (CE-AD/MS) due to the CE flow splitting, we determined the LODs for the single-detection arrangements (CE-AD and CE-MS) as well. For a fair comparison, we optimized the injection times of the single-detection

TABLE 2 CE-AD/MS, CE-AD, and CE-MS studies for the determination of theLODs and the corresponding error for $[FcMTMA]^+$ and FcMeOH ($n = 3$)

Species	$[FcMTMA]^+$		FcMeOH	
Detector	AD	MS	AD	MS
LODs (CE-AD/MS) (nM)	10 ± 2	$6{\cdot}10^2 \pm 1{\cdot}10^2$	14 ± 3	$19{\cdot}10^3 \pm 5{\cdot}10^3$
LODs (CE-AD) (nM)	9 ± 3	–	14 ± 4	–
LODs (CE-MS) (nM)	–	$5{\cdot}10^2 \pm 2{\cdot}10^2$	–	$13{\cdot}10^3 \pm 4{\cdot}10^3$

[a]The LODs were calculated for an S/N of 3.

measurements to get maximum sensitivity. The other experimental parameters were identical to the DDC. The calculated LODs for the single-detection arrangements are also listed in Table 2. Within the scope of measurement precision, the LODs of the single-detection arrangements and the DDC could be considered identical. From this, it can be concluded that there was no loss in detectability for the DDC due to the CE flow splitting.

3.4 | Determination of trimetazidine

To convict doping offenders, powerful analytical methods are needed to identify and quantify doping agents. Our new DDC has the potential to be used for that purpose as it has high sensitivity due to AD and excellent selectivity due to MS. A possible practical application for the complementary use of AD and MS is the determination of TMZ, which is usually used as a heart medication. However, its performance-enhancing effect is sometimes misused as a doping agent in competitive sports. Before the first measurement with the DDC, the electrochemical behavior of TMZ was characterized by utilizing cyclic voltammetry. The corresponding cyclic voltammograms are shown in Figure S2. For TMZ, an oxidative current was detectable above 0.8 V. According to the cyclic voltammogram, a detection potential of 1.3 V was chosen for the AD of TMZ. Additionally, the cyclic voltammogram showed the huge potential window of the ACN-based BGE. The electropherograms for the measurements with the DDC are shown in Figure 5.

It was found that TMZ could be detected with both detectors. TMZ could be identified with MS, and the m/z 267 of the protonated TMZ species was used for the data evaluation. Furthermore, under the used conditions TMZ was positively charged because it migrated before the EOF. In these experiments, MeOH was used as an EOF marker, which was added to the sample solution to increase the solubility of TMZ. However, only the AD was able to detect the added MeOH because it showed an anodic signal. The time-of-flight MS showed a too low sensitivity for m/z below 50. The depicted electropherograms (Figure 5) were recorded for a TMZ concentration

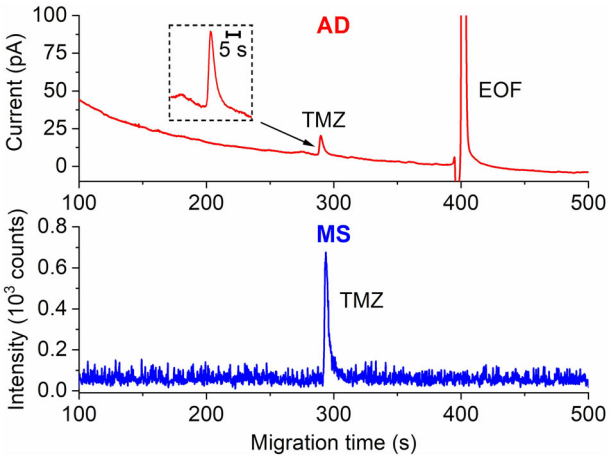

FIGURE 5 CE-AD/MS measurements of 1.25 µg/ml trimetazidine (TMZ) in BGE with 10% MeOH as sample solution. The electropherograms on top were recorded with AD (red) and at the bottom with MS (blue). Experimental parameters: detection potential AD 1.3 V (vs. Ag/AgCl) and extracted ion electropherograms for TMZ (m/z 267). The other conditions are as in Figure 2.

of 1.25 µg/ml. It could be derived from the measurements that the S/Ns for the AD were higher than for the MS. This finding was supported by the LODs, which were 0.022 ± 0.004 µg/ml for the AD and 0.6 ± 0.2 µg/ml for the MS. Therefore, the AD had about 27 times lower LODs than the MS. As TMZ belongs to the list of prohibited substances by the World Anti-Doping Agency categorized under section S 4.4, the minimum required performance limit for the analytical method is 10 ng/ml in urine (https://www.wada-ama.org/sites/default/files/resources/files/td2022mrpl_v1.0_final_eng.pdf). This is already in the order of magnitude of the LODs of the DDC. The DDC (CE-AD/MS) should reach the required performance limit with an appropriate preconcentration step included in a sample pretreatment protocol.

4 | CONCLUDING REMARKS

In this manuscript, a novel DDC for CE consisting of an AD and an MS was described for the first time. For this detector

combination with two destructive detectors, a serial detector arrangement was not possible. Hence, the CE flow was split with an FS so that the detectors could be placed in parallel to each other.

In a proof-of-concept study, we could show that the new DDC worked as the model substances could be detected at both detectors. By adjusting the height difference between AD and MS, it was possible to synchronize the detector responses. The simultaneous detection of the analytes was also an advantage over traditional DDCs with a serial detector arrangement that usually has a time offset between the detectors. It could be shown that the weaknesses of the individual detectors (AD and MS) were compensated by the complementary use of AD and MS. The AD was the method of choice for the quantification as it was found that the reproducibility of the peak areas and heights was much better for the AD than for the MS. The RSDs of both parameters were in the range of about 1% for the AD and about 10% for the MS (concentration level 0.1 mM $[FcMTMA]^+$ and 0.5 mM FcMeOH). Additionally, for our used model system, it was found that the LODs for the AD were more than three orders of magnitude lower than for the MS (calculated from the DDC LODs of FcMeOH, listed in Table 2). It has to be mentioned that the LODs of the AD depend very much on the electrochemical properties of the analyte. In contrast, the MS was the method of choice for identifying the compounds by means of the mass spectra. Furthermore, no loss in detectability was found due to the splitting as the LODs for the DDC and the single detection arrangements were identical.

Provided that the analytes are electrochemically active and detectable with MS, the DDC has the potential to solve many analytical problems. The DDC is especially interesting for applications in fields like pharmacy, environmental research, and medicine because low amounts of analytes could be precisely quantified and identified due to the complementary use of AD and MS. The practical application of the method was demonstrated by determining the doping agent TMZ. It was possible to quantify TMZ with AD and to identify the substance with MS. Overall, in this study, the potentials of the two destructive detectors (AD and MS) could be combined in an attractive DDC.

ACKNOWLEDGMENTS

We are grateful to the Deutsche Forschungsgemeinschaft (DFG, German Research Foundation) for financial support (project number MA1491/12-1).

Open access funding enabled and organized by Projekt DEAL.

CONFLICT OF INTEREST

The authors have declared no conflict of interest.

DATA AVAILABILITY STATEMENT

The data that support the findings of this study are available from the corresponding author upon reasonable request.

ORCID

Frank-Michael Matysik https://orcid.org/0000-0001-7029-1382

REFERENCES

1. Beutner A, Herl T, Matysik F-M. Selectivity enhancement in capillary electrophoresis by means of two-dimensional separation or dual detection concepts. Anal Chim Acta. 2019;1057:18–35.
2. Opekar F, Stulík K. Some important combinations of detection techniques for electrophoresis in capillaries and on chips with emphasis on electrochemical principles. Electrophoresis. 2011;32:795–810.
3. Jorgenson JW, Lukacs KD. Zone electrophoresis in open-tubular glass capillaries. Anal Chem. 1981;53:1298–302.
4. Furter JS, Boillat M-A, Hauser PC. Low-cost automated capillary electrophoresis instrument assembled from commercially available parts. Electrophoresis. 2020;41:2075–82.
5. Ramos-Payán M, Ocaña-Gonzalez JA, Fernández-Torres RM, Llobera A, Bello-López MÁ. Recent trends in capillary electrophoresis for complex samples analysis: a review. Electrophoresis. 2018;39:111–25.
6. Voeten RLC, Ventouri IK, Haselberg R, Somsen GW. Capillary electrophoresis: trends and recent advances. Anal Chem. 2018;90:1464–81.
7. Wallingford RA, Ewing AG. Capillary zone electrophoresis with electrochemical detection. Anal Chem. 1987;59:1762–6.
8. Sloss S, Ewing AG. Improved method for end-column amperometric detection for capillary electrophoresis. Anal Chem. 1993;65:577–81.
9. Holland LA, Lunte SM. Capillary electrophoresis coupled to electrochemical detection: a review of recent advances. Anal Commun. 1998;35:1–4.
10. Matysik F-M. End-column electrochemical detection for capillary electrophoresis. Electroanalysis. 2000;12:1349–55.
11. Holland LA, Chetwyn NP, Perkins MD, Lunte SM. Capillary electrophoresis in pharmaceutical analysis. Pharm Res. 1997;14:372–87.
12. Riekkola M-L. Recent advances in nonaqueous capillary electrophoresis. Electrophoresis. 2002;23:3865–83.
13. Matysik F-M. Application of non-aqueous capillary electrophoresis with electrochemical detection to the determination of nicotine in tobacco. J Chromatogr A. 1999;853:27–34.
14. Beutner A, Scherer B, Matysik F-M. Dual detection for non-aqueous capillary electrophoresis combining contactless conductivity detection and mass spectrometry. Talanta. 2018;183:33–8.
15. Olivares JA, Nguyen NT, Yonker CR, Smith RD. On-line mass spectrometric detection for capillary zone electrophoresis. Anal Chem. 1987;59:1230–2.
16. Maxwell EJ, Chen DDY. Twenty years of interface development for capillary electrophoresis-electrospray ionization-mass spectrometry. Anal Chim Acta. 2008;627:25–33.

17. Issaq HJ, Janini GM, Chan KC, Veenstra TD. Sheathless electrospray ionization interfaces for capillary electrophoresis–mass spectrometric detection. J Chromatogr A. 2004;1053:37–42.
18. Wang L, Li Y, Chen D, Da Chen DY. Electrospray ionization stability and concentration sensitivity in capillary electrophoresis-mass spectrometry using a flow-through microvial interface. Electrophoresis. 2021;42:360–8.
19. Samskog J, Wetterhall M, Jacobsson S, Markides K. Optimization of capillary electrophoresis conditions for coupling to a mass spectrometer via a sheathless interface. J Mass Spectrom. 2000;35:919–24.
20. Beutner A, Cunha RR, Richter EM, Matysik F-M. Combining C4D and MS as a dual detection approach for capillary electrophoresis. Electrophoresis. 2016;37:931–5.
21. Francisco KJM, do Lago CL. A capillary electrophoresis system with dual capacitively coupled contactless conductivity detection and electrospray ionization tandem mass spectrometry. Electrophoresis. 2016;37:1718–24.
22. Huhn C, Ruhaak LR, Mannhardt J, Wuhrer M, Neusüß C, Deelder AM, et al. Alignment of laser-induced fluorescence and mass spectrometric detection traces using electrophoretic mobility scaling in CE-LIF-MS of labeled N-glycans. Electrophoresis. 2012;33:563–6.
23. Mironov GG, Clouthier CM, Akbar A, Keillor JW, Berezovski MV. Simultaneous analysis of enzyme structure and activity by kinetic capillary electrophoresis-MS. Nat Chem Biol. 2016;12:918–22.
24. Szarka M, Szigeti M, Guttman A. Imaging laser-induced fluorescence detection at the taylor cone of electrospray ionization mass spectrometry. Anal Chem. 2019;91:7738–43.
25. Zhang D, Li W, Zhang J, Tang W, Qian C, Feng M, et al. Study on urinary metabolic profile of phenylketonuria by micellar electrokinetic capillary chromatography with dual electrochemical detection-potential clinical application in fast diagnosis of phenylketonuria. Anal Chim Acta. 2011;694:61–6.
26. Jooß K, Scholz N, Meixner J, Neusüß C. Heart-cut nano-LC-CZE-MS for the characterization of proteins on the intact level. Electrophoresis. 2019;40:1061–5.
27. Pham TTT, Mai TD, Nguyen TD, Sáiz J, Pham HV, Hauser PC. Automated dual capillary electrophoresis system with hydrodynamic injection for the concurrent determination of cations and anions. Anal Chim Acta. 2014;841:77–83.
28. Sydes D, Kler PA, Hermans M, Huhn C. Zero-dead-volume interfaces for two-dimensional electrophoretic separations. Electrophoresis. 2016;37:3020–4.
29. Böhm D, Koall M, Matysik F-M. Dead volume-free flow splitting in capillary electrophoresis. Electrophoresis. 2022;43:1438–45.
30. Matysik F-M. Special aspects of detection methodology in nonaqueous capillary electrophoresis. Electrophoresis. 2002;23:400–7.
31. Matysik F-M. Experimental characterization of end-column electrochemical detection in conjunction with nonaqueous capillary electrophoresis. Anal Chem. 2000;72:2581–6.

SUPPORTING INFORMATION

Additional supporting information can be found online in the Supporting Information section at the end of this article.

How to cite this article: Böhm D, Koall M, Matysik F-M. Combining amperometry and mass spectrometry as a dual detection approach for capillary electrophoresis. Electrophoresis. 2023;44:492–500.
https://doi.org/10.1002/elps.202200228